

Equilibrium Sampling Interval Sequences for Event-driven Controllers

Manel Velasco, Pau Martí and Enrico Bini

Abstract—Standard discrete-time control laws consider periodic execution of control jobs. Although this assumption simplifies the control design and the resource utilization analysis for later implementation, it leads to a conservative usage of computing resources. On the contrary, event-driven control offers controllers with a tighter resource utilization. However, job executions are no longer periodic, and predicting their computing requirements is crucial for efficient implementation in severely limited computing systems.

Sampling intervals for event-driven control systems show different patterns, ranging from chaotic behaviors to periodic oscillatory patterns, named equilibrium sampling interval sequences (ESIS). Focusing on resource demands predictability, in this paper we identify the conditions for event-driven controllers to exhibit ESIS, and provide methods to characterize and compute them. Finally, we study the transitions from ESIS to chaotic sampling. Simulated experiments illustrate the paper contributions.

I. INTRODUCTION

The computation load required by controllers is proportional to their rate of execution. Event-driven control systems offers controllers with a lower resource utilization than standard periodic discrete-time control laws while providing similar control performance [2]. Hence, event-driven controllers seems to be the natural choice for networked and embedded control systems with sever resource limitations. However, implementation feasibility requires to analyze their exact resource demands [3]. Unfortunately, the execution of event-driven control jobs is no longer periodic, and estimation of their computation load requires an accurate analysis.

In event-driven control systems, jobs executions are triggered by event conditions (execution rules). Generally speaking, these rules ensure that the plant will be sampled and a new control signal will be applied when the system trajectory will reach a boundary defined by a tolerated distance (or error) to the previous sampled state. Depending on several parameters such as plant, controller, boundary, and tolerated error, sampling intervals for event driven controllers show different patterns, ranging from chaotic behaviors to periodic oscillatory patterns, named equilibrium sampling interval sequences (ESIS). Note that an ESIS may determine having an event-driven controller executing periodically, but also having the controller periodically switching between two or more sampling intervals.

This work was partially supported by C3DE CICYT DPI2007-61527 and by ArtistDesign NoE IST-2008-214373.

M. Velasco and P. Martí is with the Automatic Control, Technical University of Catalonia, Pau Gargallo 5, 08028 Barcelona, Spain manel.velasco,pau.marti@upc.edu

E. Bini is with the Retis Lab, Scuola Superiore Sant'Anna, Via G. Moruzzi, 1, 56124 Pisa, Italy e.bini@sssup.it

Recent works [4], [5], [6], [3], [7], [8] on event-driven control have focused on deriving timing properties that help characterizing controllers' resource demands. In particular, given an event-driven formulation, they show how jobs activation times can be derived a priori, either using approximations or bounds.

Complementary to these results, but aligned in the same direction, this paper studies the type of activation intervals that event-driven controllers generate. First of all, we look into under which conditions event-driven controllers will exhibit ESIS. Afterwards, we provide methods to predict/compute them, when possible.

The computational load of an event-driven controller is not completely defined after predicting an ESIS. Care must be taken because not all the ESIS are desirable. In fact, ESIS can be considered *stable* or *unstable*. An event-driven controller having an unstable ESIS may eventually switch to another ESIS if its closed-loop dynamics are perturbed. Therefore, predicting an unstable ESIS does not give assurances on the controller resource demands. This problem is also covered in the paper.

Finally, as stressed before, some job activation patterns are chaotic. Therefore, it is also of great importance to study the transitions from ESIS to chaotic sampling in order to provide condition for the limits on resource demands predictability.

The rest of this paper is structured as follows. Section II establishes the event-driven control model. Sections III motivates the approach presented in the paper with an intuitive analysis of ESIS. Section IV provides the complete characterization of ESIS. Section V analyzes switching between ESIS, and to chaotic sampling. Finally, Section VI concludes the paper.

II. EVENT-DRIVEN CONTROL SYSTEM MODEL

We consider the control system

$$\begin{aligned}\dot{x}(t) &= Ax(t) + Bu(t) \\ y(t) &= Cx(t)\end{aligned}\tag{1}$$

with $x \in \mathbb{R}^{n \times 1}$, $A \in \mathbb{R}^{n \times n}$, $B \in \mathbb{R}^{n \times m}$, $u \in \mathbb{R}^{1 \times m}$, and $C \in \mathbb{R}^{1 \times n}$. Let

$$u_k = Lx(a_k) = Lx_k\tag{2}$$

be the control updates given by a linear feedback controller designed in the continuous-time domain but using only samples of the state at discrete instants $a_0, a_1, \dots, a_k, \dots$. Between control updates, $u(t)$ is held constant. In periodic sampling we have $a_{k-1} = a_k + h$, where h is the period of the controller.

The system trajectory, after the sampling time a_k , evolves according to

$$\forall t \geq a_k \quad x(t) = (\Phi(t - a_k) + \Gamma(t - a_k)L)x_k \quad (3)$$

where $\Phi : \mathbb{R} \rightarrow \mathbb{R}^{n \times n}$ and $\Gamma : \mathbb{R} \rightarrow \mathbb{R}^{n \times m}$ are defined by

$$\Phi(t) = e^{At} \quad \text{and} \quad \Gamma(t) = \int_0^t e^{As} ds B$$

Let

$$e_k(t) = x(t) - x_k \quad (4)$$

be the error evolution between consecutive samples with $t \in [a_k, a_{k+1}[$. For several types of event-driven control approaches, e.g. [4] or [7], event conditions can be generalized by introducing a generic function $f : \mathbb{R}^n \times \mathbb{R}^n \rightarrow \mathbb{R}$ that defines a boundary measuring the tolerated error with respect to the sampled state. The condition that must be ensured is

$$f(e_k(t), x_k, \Upsilon) \leq \eta \quad (5)$$

where η is the error tolerance and $\Upsilon = \{v_1, v_2, \dots, v_p\}$, $v_i \in \mathbb{R}$ is a set of free parameters. Henceforth, the considered boundaries will be restricted to

$$f(x(t) - x_k, x_k, \Upsilon) = f(x(t) - cx_k, cx_k, \Upsilon) \quad (6)$$

where $c \in \mathbb{R}$. That is, we consider boundaries that scale with the state along any direction.

Observation 1: Restriction (6) means that states having the same direction will have the same sampling interval. Note that if the sampled state scales by two, the control signal will also scale by 2 (2) and therefore the closed loop state will move twice faster. And since the boundary is twice “bigger” (6), the time taken by the state to reach it will be the same.

Hence, we can define the complete dynamics of the event-driven system by the $n + 1$ non linear discrete-time system

$$\begin{aligned} a_{k+1} &= a_k + \Lambda(x_k, \Upsilon, \eta) \\ x_{k+1} &= (\Phi(\Lambda(x_k, \Upsilon, \eta)) + \Gamma(\Lambda(x_k, \Upsilon, \eta))L)x_k \end{aligned} \quad (7)$$

where $\Lambda : \mathbb{R}^n \rightarrow \mathbb{R}$ is the solution to (1), (2), and (5) that gives the sequence $\{a_k\}$ of activation times.

A. Preliminaries

Definition 1: Let

$$h_{k+1} = \Lambda(x_k, \Upsilon, \eta) \quad (8)$$

denote the $k+1^{th}$ sampling interval as the time elapsed from a_k to a_{k+1} .

Definition 2: Let the n-equilibrium sampling interval sequence (n-ESIS)

$$\bar{h}^n = \{h_1, h_2, \dots, h_n\} \quad (9)$$

denote the periodic sequence of n consecutive sampling intervals.

From observation 1, and also similar to the approach taken in [8], the following lemma holds.

Lemma 1: For an event-driven control system (1)-(2) with (5) fulfilling (6), $\forall x_i, x_j$, if $x_i = \lambda x_j$, $\lambda \in \mathbb{R}$, then it holds that $\Lambda(x_i, \Upsilon, \eta) = \Lambda(x_j, \Upsilon, \eta)$.

Note that the inverse implication is not true. Two states having different directions can present the same sampling interval because $\Lambda^{-1}(x, \Upsilon, \eta)$ may be a multi-valuated function.

B. Example

Throughout the paper, we will illustrate the different results using the double integrator system

$$\dot{x} = Ax + Bu$$

where

$$A = \begin{bmatrix} 0 & 1 \\ 0 & 0 \end{bmatrix}, \quad B = \begin{bmatrix} 0 \\ 1 \end{bmatrix}.$$

For illustrative purposes, we will consider

$$\dot{x}_{k+}^T \dot{x}_{k+} t^2 = \eta x_k^T x_k \quad (10)$$

or

$$(x(t) - x_k)^T (x(t) - x_k) = \eta x_k^T x_k \quad (11)$$

as execution rules for triggering the control updates given by a continuous feedback law $L = [l_1 \ l_2]$. Eq. (10) intuitively mandates to trigger more frequent control updates when the state moves fast while (11) is a typical quadratic execution rule, similar to that used for example in [4]. In (10), $\dot{x}_{k+} = (A + BL)x_k$, denoting the state derivative once the controller has been applied to the sampled state.

III. 1-ESIS CHARACTERIZATION: THE MOTIVATING ANALYSIS

In many cases, for an small tolerated error, the dynamics of an event-driven control system are given by the dynamics of the continuous system. In this cases, if the eigenvalue of the continuous closed loop matrix with largest real part is real, the event-driven system will exhibit a 1-ESIS. This is condensed in the following proposition.

Proposition 1: Consider an event-driven control system (1)-(2) with (5) fulfilling (6) such that $\lim_{\eta \rightarrow 0} \Lambda(x_i, \Upsilon, \eta) = 0$. For this system, let $\lambda = \max(\text{Re}(\lambda_i))$ where $(A + BK)v_i = \lambda_i v_i$. If $\lambda \in \mathbb{R}$ and $\eta \ll 1$, then $\bar{h}^1 \approx \Lambda(v_i, \Upsilon, \eta)$.

Proof: Let the x_{k+1} dynamics of (7) be rewritten as

$$x_{k+1} = x_k + \Psi(\Lambda(x_k, \Upsilon, \eta))(A + BK)x_k \quad (12)$$

where [1]

$$\Psi(t) = \int_0^t e^{As} ds, \quad \Phi = I + A\Psi, \quad \Gamma = \Psi B$$

For $\eta \ll 1$, the time elapsed from the sampled state to reaching the boundary tends toward zero. Hence, the Taylor series of $\Psi(\cdot)$ converges, and the first order approximation is given by $\Psi(\Lambda(x_k, \Upsilon, \eta)) \approx \Lambda(x_k, \Upsilon, \eta)$. Using this approximation (12) gives

$$x_{k+1} \approx x_k + \Lambda(x_k, \Upsilon, \eta)(A + BK)x_k \quad (13)$$

Considering Lemma 1 and the system's dynamics, the system will have an 1-ESIS if $x_{k+1} = \lambda x_k$, that is, if it exists x^* such that

$$x^* + \Lambda(x^*, \Upsilon, \eta)(A + BK)x^* \approx \lambda x^* \quad (14)$$

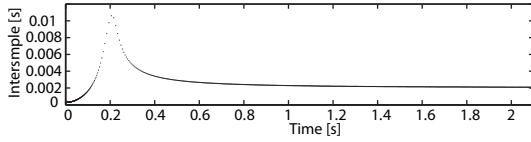


Fig. 1. Sampling interval sequence.

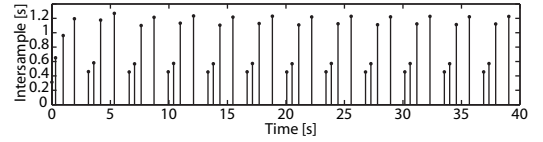


Fig. 2. Sampling interval sequence forming an 4-ESIS

Reordering (14),

$$(A + BK)x^* \approx \lambda' x^* \quad (15)$$

where $\lambda' = \frac{\lambda - 1}{\Lambda(x^*, \Upsilon, \eta)}$. Since $\lambda' \in \mathbb{R}$, it follows that $\bar{h}^1 \approx \Lambda(x^*, \Upsilon, \eta)$. ■

Proposition 1 can be read as states lying on real eigenvectors of the closed-loop system will exhibit a 1-ESIS. Note that real eigenvectors are equilibrium directions.

Example 1: Consider the double integrator system with execution rule (10) where $\eta = 0.0001$, and feedback gain $L = \begin{bmatrix} -30 & -11 \end{bmatrix}$. From (15), the eigenvectors of the closed loop system are $v_1 = \begin{bmatrix} 0.1961 & -0.9806 \end{bmatrix}^T$ and $v_2 = \begin{bmatrix} -0.1644 & 0.9864 \end{bmatrix}^T$ with $\lambda_1 = -5$ and $\lambda_2 = -6$ as eigenvalues, respectively. Taking into account that from (10) it follows that

$$\Lambda(x_k, \Upsilon, \eta) = \sqrt{\eta \frac{x_k^T x_k}{x_k^T (A + BL)^T (A + BL) x_k}}, \quad (16)$$

the dominant eigenvector gives an approximate 1-ESIS of $\bar{h}^1 = 0.0020$ seconds. To corroborate this result, Figure 1 shows the sampling interval sequence for the event-driven controller when the plant initial conditions are $x_0 = \begin{bmatrix} 0.54 & 0.84 \end{bmatrix}^T$. The x -axis is simulation time, and each control update is represented by a dot, whose height indicates the time (in seconds) elapsed to the next control update, that is, the sampling interval length. As it can be seen in the figure, the sampling sequence shows an asymptotic dynamics toward 0.00205 seconds.

IV. GENERAL n -ESIS CHARACTERIZATION

Definition 3: Let

$$\Lambda_h = \{x \in \mathbb{R}^n / \Lambda(x, \Upsilon, \eta) = h\} \quad (17)$$

be the set of points in \mathbb{R}^n having the same sampling interval.

Definition 4: Let $f_e^{(i)}(\cdot) : \mathbb{R}^n \rightarrow \mathbb{R}^n$ be the event recursive map defined as

$$\begin{aligned} f_e^{(0)}(x) &= x \\ f_e^{(1)}(x) &= (\Phi(\Lambda(f_e^{(0)}(x), \Upsilon, \eta)) + \\ &\quad \Gamma(\Lambda(f_e^{(0)}(x), \Upsilon, \eta))L)f_e^{(0)}(x) \\ f_e^{(2)}(x) &= (\Phi(\Lambda(f_e^{(1)}(x), \Upsilon, \eta)) + \\ &\quad \Gamma(\Lambda(f_e^{(1)}(x), \Upsilon, \eta))L)f_e^{(1)}(x) \\ &\vdots \\ f_e^{(i)}(x) &= (\Phi(\Lambda(f_e^{(i-1)}(x), \Upsilon, \eta)) + \\ &\quad \Gamma(\Lambda(f_e^{(i-1)}(x), \Upsilon, \eta))L)f_e^{(i-1)}(x) \end{aligned} \quad (18)$$

which recursively iterates from a given state the discrete event-driven dynamics (7) considering the corresponding sampling interval.

Definition 5: Let $F_e^{(i)}(\cdot) : \mathbb{R}^n \rightarrow \mathbb{R}^n$

$$F_e^{(i)}(\Lambda_h) = \{x \in \mathbb{R}^n / f_e^i(x_0) = x, \forall x_0 \in \Lambda_h\} \quad (19)$$

be the set of points in \mathbb{R}^n resulting from applying i -times the discrete event-driven dynamics to all points in \mathbb{R}^n having the same sampling interval

Theorem 1: If an event-driven control system (1)-(2) with (5) fulfilling (6) exhibits an n -ESIS, then it exists a Λ_h and $n \in \mathbb{R}$ such that $F_e^{(n)}(\Lambda_h) = \Lambda_h$, i.e., Λ_h is an invariant set of $F_e^{(n)}(\cdot)$.

Proof: Having n -ESIS means that there is a sampling interval sequence $\bar{h}^n = \{h_1, h_2, \dots, h_n\}$ such that $h_{n+i} = h_i$. Suppose that $F_e^{(n)}(\Lambda_{h_i}) \neq \Lambda_{h_i}$. Then $\exists x \in F_e^{(n)}(\Lambda_{h_i})$ such that $\Lambda(x) \neq h_i$, which contradicts the n -ESIS existence assumption. ■

Example 2: For standard linear discrete-time control systems with periodic sampling, $h_s, \Lambda_h = \mathbb{R}^n$. As pointed out in [6], for standard discrete-time periodic systems, the boundary that generates constant sampling is given by

$$e_k^T e_k = x_k^T Q(t) x_k \quad (20)$$

where $Q(t) = (\Phi(t) + \Gamma(t)L - I)^T (\Phi(t) + \Gamma(t)L - I)$. From (20) it follows that any controller has a 1-ESIS of $\bar{h}^1 = \{h_s\}$ because $F_e^{(1)}(\Lambda_h) = \Lambda_h$. Note that for this particular case, Λ_h is an invariant set of $F_e^{(i)}(\cdot)$, $i = 1, 2, 3, \dots$ because Λ_h is defined to be constant.

Example 3: Taking the system of example II-B with execution rule (11) with $L = \begin{bmatrix} -1 & -2 \end{bmatrix}$ and $\eta = 0.368$, it holds that $F_e^{(4)}(\Lambda_{0.4557}) = \Lambda_{0.4557}$ where $\Lambda_{0.4557} = \{\alpha[0.9865, 0.1638]^T, \alpha \in \mathbb{R}\} \cup \{\beta[0.5164, -0.8564]^T, \beta \in \mathbb{R}\}$. In fact, this system has an 4-ESIS of $\bar{h}^4 = \{0.4557, 0.5704, 1.1173, 1.2239\}$, as illustrated in Fig. 2. Therefore, $\Lambda_{0.5704}$, $\Lambda_{1.1173}$ and $\Lambda_{1.2239}$ are also invariant sets of $F_e^{(4)}(\cdot)$.

A. Determining Λ_h

For a given linear event-driven control system setup, theorem 1 is the condition of existence of an n -ESIS, but it does not provide methods to compute it. The following proposition provides a sufficient condition that permits to easily compute some n -ESIS.

Proposition 2: For an event-driven control system defined by (1)-(2) with (5) fulfilling (6), if $\exists \lambda \in \mathbb{R}$ and $x^* \in \mathbb{R}^n$ such that $\lambda x^* = f_e^{(i)}(x^*)$, then $\Lambda_h = \{x \in \mathbb{R}^n / \Lambda(x, \Upsilon, \eta) = \Lambda(x^*, \Upsilon, \eta)\}$.

Proof: If $\lambda x^* = f_e^{(i)}(x^*)$, then x^* is an eigenvector of $f_e^{(i)}(\cdot)$ and thus its direction does not change, i.e., it's an equilibrium direction. By lemma 1 it holds that all points in the line λx^* have the same period. ■

Observation 2: The problem of finding equilibrium directions given by Proposition 2 may be read as finding the equilibrium points of the projection of the event-driven dynamics given by $f_e^{(i)}(\cdot)$ onto an sphere. The projection of the dynamics is found by applying

$$\begin{aligned} \Pi : \mathbb{R}^n &\rightarrow S^{n-1} \in \mathbb{R}^n \\ x &\rightarrow \Pi(x) = \frac{x}{|x|} \end{aligned} \quad (21)$$

to $f_e^{(i)}$. The resulting function $\Pi f_e^i = \Pi(f_e^{(i)})$ describes how the orientation of the state x changes at each iteration by associating each state direction to a point in S^{n-1} . The application of (21) to the premise of proposition 2, that is,

$$\Pi(\lambda x^*) = \Pi(f_e^{(i)}(x^*)), \quad (22)$$

transforms to

$$\bar{x}^* = \Pi f_e^{(i)}(\bar{x}^*). \quad (23)$$

Therefore finding equilibrium directions for an event-driven control system is equivalent to finding equilibrium points of $\Pi f_e^{(i)}(\cdot)$.

Being a sufficient condition, Proposition 2 will not capture all the possible n-ESIS. In fact, we conjecture that it is unable to capture n-ESIS of event-driven control systems when there are limit cycles in $\Pi f_e^k(\cdot)$.

Example 4: Consider a standard linear discrete-time control system with periodic sampling h_s , of dimension $n = 2$. Consider a controller L that locates complex conjugated discrete poles in the closed-loop discrete dynamics. In this situation, $\Pi f_e^k(\cdot)$ has no equilibrium points and proposition 2 will fail at finding h_s . However, the theorem is able to determine its existence (as illustrated in example 2).

Taking into account lemma 1, proposition 2 and observation 2, we can derive a graphical interpretation of n-ESIS for second order system (see Figures 3 and 4). Consider the diagram where the variable of interest is the state vector orientation. In this bi-dimensional state space, we represent S^1 by the interval $[0, 2\pi]$. The diagram has two curves generated by 1-map defined as $\theta_{k+1} : [0, 2\pi] \rightarrow [0, 2\pi]$ such that $\theta_{k+1} = \arg[(\Phi(\Lambda(x_k)) + \Gamma(\Lambda(x_k))L) [\cos(\theta_k) \sin(\theta_k)]]$. This map shows how the orientation evolves at each step as function of the previous orientation. The first curve is generated by the 1-map $\forall \theta_0 \in [0, 2\pi]$, that is, it gives all possible transitions between consecutive orientations, for all orientations. The second curve, with a squared shape, only gives the transitions between consecutive orientations from a given initial orientation. When the squared curve visits a point in the other curve (or in the diagonal) two times, an n-ESIS is identified. Moreover, n will be the number of visited intermediate points before revisiting the same point, making an n-cycle orbit.

Example 5: Consider the diagram for example 3 shown in Figure 3. As it can be seen, the squared curve starting

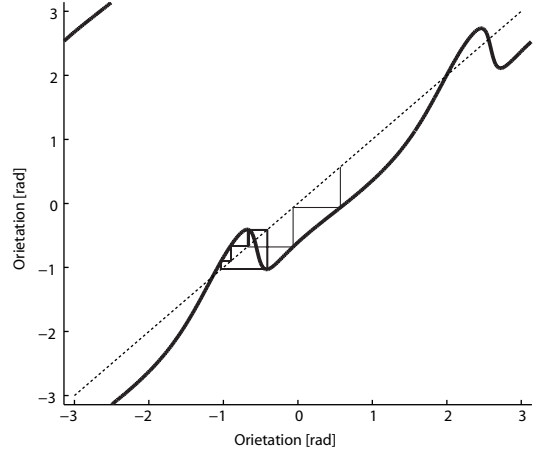


Fig. 3. 1-dimension maps for the orientation of the event driven control system dynamics

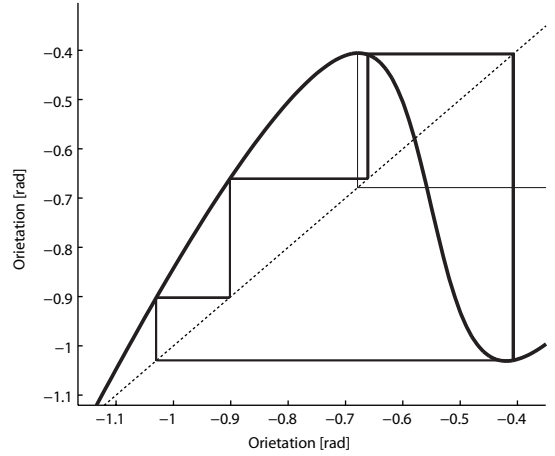


Fig. 4. Zoom in of the previous figure.

near $[0.8, 0.8]$ evolves to a 4-cycle orbit. This fact can be better observed in the detailed plot 4.

B. Stability of n-ESIS

Theorem 1 and proposition 2 do not differentiate between stable and unstable n-ESIS. Consider that the starting point of a given event-driven dynamics belongs to an unstable n-ESIS. Although the dynamics will stick to this sampling sequence, a minimal perturbation may provoke to switch to another dynamics governed by an stable n-ESIS. From a resource utilization predictability point of view, this situation is extremely undesirable. Predicting the computation load of the controller in the unstable n-ESIS does not guarantee feasibility of the implementation because suddenly the controller may demand a different load if a switch to an stable n-ESIS occurs. Therefore, it is of interest to study whether n-ESIS are stable or not.

The stability analysis of the set Λ_h of $F_e^{(n)}(\cdot)$ using the theory of invariant sets for discrete maps applied to (7) is left

for future work. However, taking advantage of proposition 2, we can easily characterize the stability of the n-ESIS generated by equilibrium directions.

Proposition 3: For an event-driven control system defined by (1)-(2) with (5) fulfilling (6), an n-ESIS obtained by proposition 2 will be stable if the eigenvalues of

$$\left| \frac{\partial \Pi f_e^{(i)}(x)}{\partial x} \right|_{x^*} \quad (24)$$

are less than one in absolute value.

Proof: It follows from observation 2 and the application of the Lyapunov indirect method. ■

Observation 3: Note that when the eigenvalues of the Jacobian (24) are larger than one in absolute value, the n-ESIS will be unstable. Those equal to 1 in absolute value require a deeper analysis.

Example 6: Taking again example 3, we study whether its 4-ESIS are stable and unstable. Starting from the equation

$$\lambda x^* = f_e^{(4)}(x^*) \quad (25)$$

we can compute its solutions, which gives 8 4-ESIS. By applying proposition 3 we can conclude that 4 of them are stable. In particular, we identified an 4-ESIS for $\lambda_{0.4557}$. The Jacobian matrix (24) for this system at $x \in \Lambda_{0.4557}$ is

$$J = \begin{bmatrix} 0.4238 & 0.2556 \\ -0.2909 & -0.1754 \end{bmatrix}. \quad (26)$$

And its eigenvalues are $\lambda_1 = 0$ and $\lambda_2 = 0.2448$, that are less than 1 in absolute value. Therefore, the 4-ESIS $h^4 = \{0.4557, 0.5704, 1.1173, 1.2239\}$ is stable.

V. BIFURCATIONS

After characterizing n-ESIS, from a controller resource utilization point of view, it is of interest to study when the event-driven closed loop dynamics jumps from one n-ESIS to an m-ESIS when a "parameter" varies, for example, as a function of the tolerated error η . This can be assessed by applying bifurcation theory, e.g. [9] or [10]. Our first concern is to study how small variations in η affect n-ESIS. Afterward, we will study under which conditions the event-driven dynamics jump from one n-ESIS to another.

The equilibrium directions of the event-driven dynamics are the equilibrium points of its projection on the sphere, which are the solutions of

$$G(x, \eta) = \Pi f_e^{(i)}(x, \eta) - \Pi x = 0. \quad (27)$$

For the sake of clarity, in (27) we explicitly show the dependency of $f_e^{(i)}(\cdot)$ on η .

Proposition 4: For an event-driven control system defined by (1)-(2) with (5) fulfilling (6), the evolution of an n-ESIS obtained by proposition 2 with respect to small changes in η is

$$\delta x^* = \left(\frac{\partial G}{\partial x} \right)^{-1} \frac{\partial G}{\partial \eta} \delta \eta. \quad (28)$$

Proof: According to proposition 2 and observation 2, n-ESIS are generated by equilibrium points of the event-driven

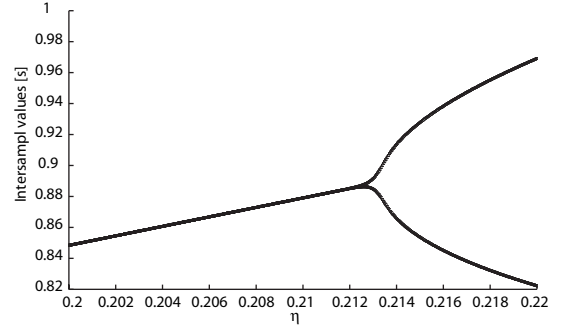


Fig. 5. Bifurcation of the example 7

dynamics projected over the sphere. Such equilibrium points are the solutions of (27). For some η , given an equilibrium point x^* , it holds that $G(x^*, \eta) = 0$. If we vary a little bit η with $\delta \eta$, the corresponding variation on $x = x^* + \delta x^*$ should also fulfil (27). Therefore, the first Taylor approximation on this variation is

$$G(x^* + \delta x^*, \eta + \delta \eta^*) = G(x^*, \eta) + \frac{\partial G}{\partial x} \delta x^* + \frac{\partial G}{\partial \eta} \delta \eta = 0,$$

which yields to (28). ■

Observation 4: Equation (28) describes how the n-ESIS evolves as η slightly changes. Given the equilibrium state, that is, given an starting direction and sampling interval $\Lambda(x^*)$, we can compute \bar{h}^n and we can assess how \bar{h}^n changes as η slightly changes. This permits to determine the computational load of a controller depending for example on η , that is, it permits to perform resource utilization analysis as a function of η .

To study when a given event-driven dynamics jumps from one n-ESIS to an m-ESIS, we have to look when stable equilibrium points of the projection of the dynamics on the sphere are no longer stable. Looking at (28), it will be not well defined when $\left(\frac{\partial G}{\partial x} \right)$ loses its rank, that is, when its eigenvalues are zero. In this case, one or more eigenvalues of (24) reach the unit circle. That is, stability is lost. At this point a bifurcation occurs, and the event-driven dynamics jump to another n-ESIS. The type of bifurcation depends on how many eigenvalues crosses the unit circle, and how they cross it. There is a very extensive literature on this topic to perform the analysis, see e.g. [10].

Example 7: Consider again example 3 with η in the range $[0.20, 0.22]$. This system presents an 1-ESIS at $\eta = 0.20$ and a 2-ESIS at $\eta = 0.22$. Therefore, the Jacobian of the map $\Pi f_e^{(1)}(\cdot)$ presents an eigenvalue that crosses the unit circle towards outside, while the Jacobian of $\Pi f_e^{(2)}$ presents one or more eigenvalues that go inside the unit circle, having then all of them inside. Therefore, the 2-ESIS will be stable. The corresponding values for the jacobians are

$$J_{\eta=0.2, x^*=[0.8 \ -0.56]^T}(\Pi f_e^{(1)}) = \begin{bmatrix} 0.2291 & 0.3347 \\ -0.6567 & -0.9671 \end{bmatrix}$$

$$J_{\eta=0.22, x^*=[0.84 \ -0.53]^T}(\Pi f_e^{(2)}) = \begin{bmatrix} 0.0149 & 0.0234 \\ 0.2716 & 0.4265 \end{bmatrix},$$

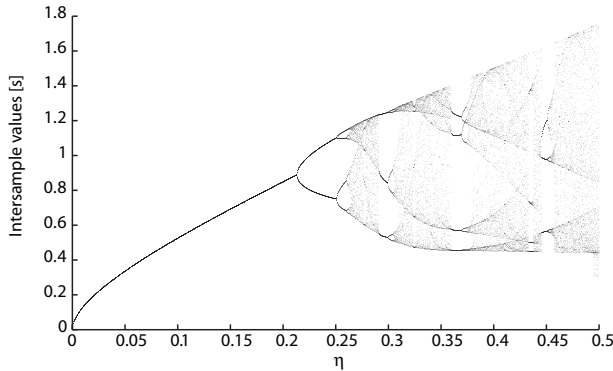


Fig. 6. Bifurcation diagram for double integrator with boundary (11).

both with eigenvalues inside the unit circle. Figure 5 presents a graphical representation of the stable n -ESIS as function of the parameter η in the specified range. It can be appreciated that a bifurcation appears at $\eta = 0.213\dots$, between the identified n -ESIS. Before this bifurcation point, within the 1-ESIS, observe that as η increments, the longer is the sampling interval. This type of figure will be further explained next.

A. Transition to chaos and the endless resource demand analysis problem

Parallel to studying transitions from an n -ESIS to an m -ESIS, it is also of interest to study whether the transition brings the event-driven control system to chaotic sampling. The type of boundary, and how its parameters are selected, may determine transitions to chaotic sequences of sampling intervals. Achieving this scenario means that predicting computational demands of controllers is no longer possible.

A dynamical system must have the following properties [11] to be classified as chaotic:

- 1) it must be sensitive to initial conditions,
- 2) it must be topologically mixing, and
- 3) its periodic orbits must be dense.

These conditions may be checked before selecting the boundary or its parameters. For example, for the case of event-driven control systems where control updates are generated by (20), that is, for periodic sampling, the first property does not hold, and therefore we can “obviously” affirm that no chaotic sampling will appear.

Although the formal analysis is left for future work, the next example illustrates some interesting concepts in terms of controller resource demand analysis.

Example 8: Consider again example 3 where control updates were generated by boundary (11). In order to prove for example that (11) generates chaos it suffices to show that the projection of the generated event-driven dynamics onto the sphere, which is a 1-map, will present an 3-ESIS [12]. Figure 6 shows the last sampling interval sequences after 10000 iterations of the event-driven closed-loop system as a function of η (Figure 5 belongs to this figure). By simple inspection, we can observe that for $\eta = 0.298$, a 3-ESIS is found. Figure 6 also shows that for small values

of η the system has an unique stable 1-ESIS, which becomes longer as the boundary is larger, i.e., as η grows. At point $\eta = 0.213\dots$ (as previously stated in example 7) there is a doubling sampling interval bifurcation, which makes the system to jump to a 2-ESIS. In fact the 1-ESIS found before this jump is still there, but has become unstable. Progressing with η , there is a second double bifurcation at $\eta = 0.251\dots$ And once again at $\eta = 0.2645$, and so on until the sampling sequence is considered chaotic. The transition to chaos is not only a crossover barrier. Inside the chaotic area there are stable n -ESIS. For example at $\eta = 0.298$, inside the chaotic zone, we find an stable 3-ESIS. Observe that there is also a relative long 4-ESIS (the one identified in example 3) at $\eta = 0.368$. It is worth noting that the relation of the different bifurcations in one dimensional map (as for example in Figure 6) is related to the Feigenbaum constant. It permits to predict the point ($\eta = 0.271\dots$) at which the system dynamics will switch to chaos.

VI. CONCLUSIONS

This paper tackles the problem of identifying which type of sampling intervals will an event-driven control system exhibit. This permits to predict controller resource demands and thus implement efficient control systems in platforms with severe limited resources. The analysis shows when periodic sampling interval sequences exists, and also covers the problem of transitions to chaos. Future work will develop the formal analysis for event-driven systems applying symbolic dynamics from chaos theory.

VII. ACKNOWLEDGMENTS

This work was partially supported by C3DE CICYT DPI2007-61527, and by ArtistDesign NoE IST-2008-214373.

REFERENCES

- [1] K.J. Åström and B. Wittenmark, *Computer controlled systems*, Prentice Hall, 1997.
- [2] W.P.M.H. Heemels, J.H. Sandee, and P.P.J. van den Bosch, Analysis of event-driven controllers for linear systems, *International Journal of Control*, 81(4), 2008, pp. 571-590.
- [3] M. Velasco, P. Martí and E. Bini, “Control-driven Tasks: Modeling and Analysis”, in *29th IEEE Real-Time Systems Symposium*, 2008.
- [4] P. Tabuada, Event-triggered real-time scheduling of stabilizing control tasks, *IEEE Trans. on Automatic Control*, 52(9), 2007, pp. 1680-1685.
- [5] M. Lemmon, T. Chantem, X. S. Hu, and M. Zyskowski, “On self-triggered full information h -infinity controllers,” in *Proceedings of the 10th International Conference on Hybrid Systems: Computation and Control*, Pisa, Italy, Apr. 2007.
- [6] M. Velasco, P. Martí, and C. Lozoya, “On the timing of discrete events in event-driven control systems,” in *Proceedings of the 11th International Conference on Hybrid Systems: Computation and Control*, St. Louis, USA, Apr. 2008.
- [7] X. Wang and M. Lemmon, Self-triggered Feedback Control Systems with Finite-Gain L_2 Stability, *IEEE Transactions on Automatic Control*, to appear, 2008.
- [8] A. Anta and P. Tabuada, “Self-triggered stabilization of homogeneous control systems”, in *2008 American Control Conference*, 2008.
- [9] K.T. Alligood, *Chaos: an introduction to dynamical systems*, Springer-Verlag New York, LLC., 1997.
- [10] R.L. Devaney, *An Introduction to Chaotic Dynamical Systems*, 2nd ed., Westview Press, 2003.
- [11] B. Hasselblatt and A. Katok, *A First Course in Dynamics: With a Panorama of Recent Developments*, Cambridge University Press, 2003.
- [12] T.-Y. Li and J.A. Yorke, Period Three Implies Chaos, *The American Mathematical Monthly*, Vol. 82, No. 10., Dec. 1975, pp. 985-992.